



HAL
open science

Impact of temperature on *Marinobacter hydrocarbonoclasticus* SP17 morphology and biofilm structure during growth on alkanes

Priscilla Branchu, Alexis Canette, Sara Medina Fernandez, Julie Mounier, Thierry Meylheuc, Romain Briandet, Régis Grimaud, Murielle Naitali

► **To cite this version:**

Priscilla Branchu, Alexis Canette, Sara Medina Fernandez, Julie Mounier, Thierry Meylheuc, et al.. Impact of temperature on *Marinobacter hydrocarbonoclasticus* SP17 morphology and biofilm structure during growth on alkanes. *Microbiology*, 2017, 163, pp.669-677. 10.1099/mic.0.000466 . hal-01606511

HAL Id: hal-01606511

<https://hal.science/hal-01606511v1>

Submitted on 19 Mar 2021

HAL is a multi-disciplinary open access archive for the deposit and dissemination of scientific research documents, whether they are published or not. The documents may come from teaching and research institutions in France or abroad, or from public or private research centers.

L'archive ouverte pluridisciplinaire **HAL**, est destinée au dépôt et à la diffusion de documents scientifiques de niveau recherche, publiés ou non, émanant des établissements d'enseignement et de recherche français ou étrangers, des laboratoires publics ou privés.

Copyright

Impact of temperature on *Marinobacter hydrocarbonoclasticus* SP17 morphology and biofilm structure during growth on alkanes

Priscilla Branchu,^{1,*†} Alexis Canette,¹ Sara Medina Fernandez,² Julie Mounier,² Thierry Meylheuc,¹ Romain Briandet,¹ Régis Grimaud² and Murielle Naïtali³

Abstract

Alkanes are widespread pollutants found in soil, freshwater and marine environments. *Marinobacter hydrocarbonoclasticus* (*Mh*) strain SP17 is a marine bacterium able to use many hydrophobic organic compounds, including alkanes, through the production of biofilms that allow their poor solubility to be overcome. This study pointed out that temperature is an environmental factor that strongly affects the biofilm formation and morphology of *Mh* on the model alkanes, hexadecane and paraffin. We showed that *Mh* biofilm formation and accumulation of intracytoplasmic inclusions are higher on solid alkanes (hexadecane at 10 °C and paraffin at 10 °C and 30 °C) than on liquid alkane (hexadecane at 30 °C) or soluble substrate (lactate at both temperatures). We also found that *Mh* produces more extracellular polymeric substances at 30 °C than at 10 °C on alkanes and none on lactate. We observed that bacterial length is significantly higher at 10 °C than at 30 °C on lactate and hexadecane. On paraffin, at 30 °C, the cell morphology is markedly altered by large rounded or irregularly shaped cytoplasmic inclusions. Altogether, the results showed that *Mh* is able to adapt and use alkanes as a carbon source, even at low temperature.

INTRODUCTION

Alkanes are widespread in the environment, including freshwater and marine ecosystems. They have diverse origins such as crude oil spills, natural oil seeps and organisms like plants, algae and bacteria [1]. These compounds represent a large pool of potential carbon and energy sources but their weak water solubility results in poor mass transfer to microbial cells. However, their biodegradation by micro-organisms is well-established. The bacteria that are able to metabolize them are collectively referred to as hydrocarbonoclastic bacteria (HCB) [2, 3]. To overcome the poor solubility of alkanes, HCB have developed two major strategies [4, 5]: (i) biofilm formation at the water–hydrophobic organic compound (HOC) interface [6–8]; and (ii) biosurfactant production [9]. Biofilm formation on HOCs is thus recognized as an important strategy used by HCB to overcome the low solubility of their substrates. Indeed, it would permit direct contact between bacteria and hydrocarbons [10] and likely direct uptake from the

hydrocarbon phase, although the latter hypothesis remains to be tested. In the case of *Pseudomonas* species [11], direct internalization of biosurfactant-covered hydrocarbon droplets has been hypothesized. Regardless of the accession mechanism, alkanes are then utilized as a source of carbon and energy, or stored as lipid inclusions within cells. A number of species accumulate lipid inclusions, with various compositions [12]. The mechanism of lipid storage formation within prokaryotic cells is likely to involve the plasma membrane that initiates small lipid droplets, which conglomerate to form membrane-bound lipid pre-bodies. Thereafter, these lipids are released in the cytoplasm [12].

Marinobacter species have been found in various marine environments, including pristine and oil-contaminated seawater, Arctic ice, deep-sea sediment and the seafloor [13–17]. They belong to the HCB group and can participate in the recycling of HOC [18]. Among these, *Marinobacter*

Received 8 March 2017; Accepted 23 March 2017

Author affiliations: ¹Micalis Institute, INRA, AgroParisTech, Université Paris-Saclay, 78350 Jouy-en-Josas, France; ²CNRS/Univ Pau & Pays Adour, Institut des Sciences Analytiques et de Physico-Chimie pour l'Environnement et les Matériaux, UMR5254, 64000, Pau, France; ³Micalis Institute, AgroParisTech, INRA, Université Paris-Saclay, 78350 Jouy-en-Josas, France.

*Correspondence: Priscilla Branchu, priscilla.branchu@inserm.fr

Keywords: temperature; biofilm; poorly soluble substrate; lipid inclusion; cell shape; *Marinobacter*; physical state of the substrate/substratum.

Abbreviations: ANOVA, analyses of variance; CLSM, confocal laser scanning microscopy; HCB, hydrocarbonoclastic bacteria; HOC, hydrophobic organic compound; *Mh*, *Marinobacter hydrocarbonoclasticus*; SEM, scanning electron microscopy; SSW, synthetic seawater; TEM, transmission electron microscopy.

†Present address: IRSD, Université de Toulouse, INSERM, INRA, ENVT, Toulouse, France.
One supplementary figure is available with the online Supplementary Material.

hydrocarbonoclasticus (*Mh*) strain SP17 was isolated from sediment of the Mediterranean Sea in the Gulf of Fos (French Mediterranean coast) [19]. *Mh* SP17 is known to utilise alkanes (C₈ to C₂₈), long-chain fatty alcohols and acids, wax esters and triglycerides as sole carbon sources. *Mh* SP17 forms biofilms at the HOC–water interface [20–22] in laboratory experiments performed at 30 °C. At this temperature, growth on hexadecane involves an alteration of *Mh* SP17 physiology, as demonstrated by the global changes in gene expression profiles [22–24].

Temperature is an important abiotic factor known to influence biofilm formation in some bacterial species [8, 25–27]. To our knowledge, the effect of temperature on alkane uptake has not been thoroughly investigated in *Mh* SP17. Most laboratory studies with *Mh* SP17 have been performed at 30 °C, the optimum growth temperature [20, 22, 24], but that is higher than the temperatures encountered in the Mediterranean Sea, where it can be as low as 10 °C. The aim of this study was to determine the impact of temperature on biofilm formation and architecture as well as cell morphology during the growth of *Mh* SP17 derivative strains on alkanes. Two models of alkanes were chosen, hexadecane and paraffin, with solidifying points of 16 and 55 °C, respectively.

METHODS

Bacterial strains and pre-culture conditions

Strain JM1 is a spontaneous streptomycin-resistant mutant isolated from the original isolate *Marinobacter hydrocarbonoclasticus* SP17 ATCC 49840 [19, 23]. The MJ6-1 strain [23] is a fluorescent derivative of SP17 constructed by insertion of the mini-Tn7T-Tp-eyfp [28]. The strains were stored in 20 % glycerol in synthetic seawater (SSW) [19] at –80 °C. They were pre-cultivated for 1 day in SSW supplemented with 20 mM lactate (lactate SSW; 30 °C, orbital shaking at 180 r.p.m.). They were then diluted at 2 % (v/v) in fresh lactate SSW and grown in the same conditions overnight.

Biofilm growth

Bacterial cells were harvested by centrifugation (10 000 g, 20 °C, 15 min), washed once and diluted to a final optical density at 600 nm (OD₆₀₀) of 0.01 in SSW. Lactate (20 mM) or hexadecane (2 % v/v) were added directly to the cell suspensions, whereas the paraffin was used as thin strips (cut with microtome at 15 µm thickness) and stuck on solid supports by heating (10 min at 45 °C). Cultures were grown at 10 or 30 °C in static conditions in flasks or plates depending on the downstream analyses. Thereafter, biofilms were quantified by crystal violet staining assay or observed and analysed by using microscopy techniques.

Crystal violet staining assays

The MJ6-1 biofilms were first grown as described above in Bioscreen microplates (Labsystems, France) for up to 20 days. The Bioscreen microplates are specifically designed to avoid evaporation during long experiments. Samples were sacrificed at each time point. The biofilms were stained by crystal violet (0.2 % v/v) and then washed three times

with deionised water. The residual crystal violet was solubilized with an ethanol solution (50 %). Then, the absorbance was read at 600 nm on an automated Bioscreen C analyser (Labsystems), after dilution when necessary, and is referred to as CV_{OD600} in the text. Nine wells were measured for each data point (three replicates of three independently grown cultures). Three wells per plate containing non-inoculated medium were used for blank subtraction.

Scanning electron microscopy (SEM)

MJ6-1 bacteria cells were inoculated and grown as described above in 24-well plates containing aluminium solid supports. After incubation (5 and 14 days at 30 or 10 °C, respectively), samples were fixed in 0.15 M cacodylate buffer containing 2.5 % (v/v) glutaraldehyde (pH 7.4) for 1 h at room temperature followed by overnight incubation at 4 °C. Samples were then washed three times for 5 min with 0.15 M sodium cacodylate buffer. Samples were dehydrated with increasing concentrations of ethanol at room temperature (50 % v/v for 30 min, then 70, 90 and 100 % (twice) v/v for 10 min at each step). Samples were critical-point dried (Quorum Technologies K850, Elexience, France) at 75 bar and 37 °C with liquid CO₂ as the transition fluid and then depressurized slowly (400 cm³ min⁻¹). Each aluminium support carrying the sample was mounted on an aluminium stub with double-sided tape. Samples were sputter-coated (Polaron SC7640, Elexience) in Ar plasma with Pt (approximately 30 nm thick) at 10 mA and 0.8 kV over a duration of 200 s. Observations were performed in a field-emission SEM S4500 (Hitachi, Japan) in high vacuum, with a low secondary electron detector, at 2 kV and 16 mm working distance. The sample holder tilt was 45 °C.

Transmission electron microscopy (TEM)

JM1 biofilms were inoculated and grown on paraffin in Petri dishes as described above. TEM experiments were performed on the total bacteria (i.e. both planktonic bacteria detached from the biofilm and biofilm-embedded bacteria) or only on *in situ* structured biofilm. The total bacteria were collected and pelleted at 3 200 g for 10 min at room temperature. Thereafter, bacteria were fixed for 1 h at room temperature and overnight at 4 °C in a 0.15 M cacodylate buffer containing 2.5 % (v/v) glutaraldehyde (pH 7.4). After washing three times for 5 min with 0.15 M cacodylate buffer, the bacteria were post-fixed for 1 h in 1 % (v/v) osmium tetroxide in 0.15 M cacodylate buffer (pH 7.4) and washed twice for 10 min with distilled water at room temperature. For the *in situ* structured biofilm cells, the samples were prepared and observed according to the method described by Canette *et al.* [29]. Briefly, the fixation was performed as described above, directly on the biofilm-embedded cells after removal of the culture medium. The fixed biofilm was then pre-embedded in a 2.5 % agarose solution maintained above its gelling point at 50 °C. The agarose layer with the sample was detached from the paraffin and cut into small pieces, taking care to maintain its orientation. Thereafter, the fixed cells (agarose-embedded or not, depending on the sample) were dehydrated in an ethanol series [30, 50, 70, 90 and 100 % (twice) v/v, 10 min for each step]. For

the total bacteria samples, we added a 10 min intermediate bath in propylene oxide before the next step. Then, bacteria were impregnated at room temperature in successive mixes of EPON resin/ethanol (for the *in situ* structured biofilm) or EPON resin/propylene oxide (for total bacteria): 1 : 2 for 20 min; 1 : 1 overnight; 2 : 1 for 1 h; twice in pure EPON for 1 h. The polymerization was induced by incubation for 17 h at 60 °C. Ultrathin sections of 90 nm were cut with an ultramicrotome (OMU3, Reichert, Germany) and deposited on 200 mesh copper grids. Sections were stained for 30 min in oolong tea extract [0.05 % (w/v) in distilled water (Eloise, France)]. Samples were observed at 75 kV with an H-600 TEM (Hitachi, Japan) equipped with a 1024×1024 pixel format Orca charge-coupled device camera (Hamamatsu, Japan) driven by AMT Image Capture Engine software (version 5.42).

Confocal laser scanning microscopy (CLSM)

MJ6-1 biofilms were inoculated and grown on paraffin in Petri dishes as described above. The paraffin thickness (15 µm) permitted the observation of the biofilms directly through the paraffin on a motorized stage of an inverted Leica TCS SP8 AOBS confocal microscope (Leica Microsystems, Germany) using a 40× water immersion optical lens with a free working distance of 3.3 mm (HCX APO L, 0.80 NA, W U-V-I, Leica, Germany). Yfp produced by bacteria was excited at 488 nm using an argon laser (30 % intensity, acoustico-optical tunable filter at 5 %) and the emitted fluorescence was recorded between 520 to 600 nm with a HyD detector with the gain set at 70 %. Four stacks of *xy* images with a *z*-step of 1 µm were acquired for each sample at 600 Hz speed. Projections of surface-associated bacteria were reconstructed from *z*-series images using the Easy 3D function (in blend mode) of IMARIS 7.7.2 software (Bitplane, Switzerland). Biovolumes were calculated with the Surpass function of IMARIS 7.7.2 and the Batch Coordinator 1.1.1 software extension. To calculate substratum coverage on paraffin, images were analysed with a home-made Java script [30] executed by ICY, an open-source image analysis platform [31].

To observe lipid inclusions and measure the bacteria lengths, biofilms of JM1 were grown on thin strips of paraffin stuck on microscopic slides within a Petri dish. Following growth, biofilms were stained with the red nucleic acid dye, Syto61 (1 : 1000) and the green lipophilic dye BODIPY (0.05 mg ml⁻¹S-11343 and D-3922, respectively, Life Technologies, France) and observed upside-down under the CLSM. Bacteria lengths or diameter were measured on the Syto61 or BODIPY channel, respectively, by using Leica software LAS AF 3.2 on 50 cells from three images for each condition. Single focal plane images were processed using Fiji [32] (<https://fiji.sc/>) to merge channels, make scale bars and calculate lipid inclusion areas (using watershed segmentation on binarized images).

Statistical analysis

Analyses of variance (ANOVA) were performed using Statgraphics software (Manugistics, Maryland, USA). *P* values tested the statistical significance of each of the factors by

means of *F* tests. When *P* values were less than 0.05, these factors had a statistically significant effect at a 95 % confidence level. Student's *t*-test was used for bacteria length comparison.

RESULTS AND DISCUSSION

Among several factors, the temperature appears to be the most impacting factor for biofilm production by *Mh*

A preliminary study was performed to point out important factors for MJ6-1 biofilm production on insoluble substrates. We first tested the impact of the cell density ($OD_{600}=0.1$ or 0.01), the physiological state of the inoculum (exponential growth or stationary phase), the NaCl concentration (0.2 M NaCl, the usual concentration reported in the literature or 0.6 M to be closer to the seawater salinity) and the temperature (20, 25 or 30 °C) on the biomass production as a biofilm after 48 h of incubation, using crystal violet staining. The cell density and the growth phase of the inoculum had no significant impact on biofilm production (Table 1 – First set of experiments). As such, they underwent no further consideration and were set at the values indicated in the Methods section. The salinity and temperature did influence biofilm formation. Growth under 0.6 M salinity ($CV_{OD600}=1.57$) or at 20 °C ($CV_{OD600}=1.56$) significantly increased ($P<0.05$) biofilm formation compared to growth at 0.2 M salinity ($CV_{OD600}=0.97$) or at 30 °C ($CV_{OD600}=0.90$ Table 1 – First set of experiments). As the Mediterranean Sea has an average temperature lower than 20 °C, in a second set of experiments, we tested the impact of lower temperature of incubation (10, 15 and 20 °C) at salinities of 0.2 or 0.6 M on the biofilm biomass after 7 days. Surprisingly, we observed increased biofilm formation at 10 °C ($CV_{OD600}=3.39$) in relation to 15 °C ($CV_{OD600}=2.28$) and 20 °C ($CV_{OD600}=1.83$), whereas the salinity had no significant impact at these temperatures (Table 1 – Second set of experiments).

As such, from this preliminary study, the temperature appeared to be a critical environmental factor for *Mh* biofilm formation. We therefore decided to focus on the effect of temperature by comparing biofilm growth at 10 or 30 °C on the non-soluble carbon sources hexadecane (solid at 10 °C and liquid at 30 °C) or paraffin (solid at both temperatures). Lactate was employed as a control soluble carbon source. The salinity, having no impact at low temperature, was set at 0.2 M NaCl, as in most of published reports [20, 22, 24].

Growth temperature influences biofilm formation and spatial organization on alkanes

We determined the kinetics of biofilm formation by MJ6-1 on hexadecane and paraffin at 10 and 30 °C by crystal violet staining. *Mh* only produced a large amount of biofilm when grown at 30 °C with paraffin and at 10 °C with paraffin or hexadecane (Fig. 1). On hexadecane, biofilm overproduction at 10 °C in comparison with 30 °C was transient, implying a decrease in biomass that could be linked to cell detachment or biofilm shedding after 14 days. Although biofilm formation was

Table 1. Screening of important factors for biofilm formation of *Mh*

	First set of experiments – 48 h growth			Second set of experiments – 7 days growth	
		CV _{OD600 nm}	ANOVA group	CV _{OD600 nm}	ANOVA group
Carbon source	Lactate	1.96	A	2.42	B
	Hexadecane	1.80	A	2.67	B
	Acetate	0.81	B	2.56	B
	Paraffin	NT	NA	3.93	A
	None	0.50	C	0.91	C
Initial OD _{600 nm}	0.1	1.33	A	NT	NA
	0.01	1.20	A	NT	NA
NaCl concentration	0.6 M	1.57	A	2.72	A
	0.2 M	0.97	B	2.28	A
Physiological state of inoculum	Stationary	1.30	A	NT	NA
	Exponential	1.24	A	NT	NA
Temperature	10 °C	NT	NA	3.39	A
	15 °C	NT	NA	2.28	B
	20 °C	1.56	A	1.83	C
	25 °C	1.34	B	NT	NA
	30 °C	0.90	C	NT	NA

CV_{OD600 nm} is the mean of all the results obtained for each given condition, independently of other factors, from three biological repeats after 48 h (first set of experiments) or 7 days (second set of experiments). The ANOVA group obtained after the statistical test is also specified. NT, not tested; NA, non-applicable.

previously shown to be essential for *Mh* SP17 hexadecane uptake [20], we can speculate that cells detach continuously from the biofilm, which remains thin. In agreement, Klein *et al.* [20] showed that cells of *Mh* SP17 came off the biofilm when grown on hexadecane at 30 °C. In addition to detachment, the difference in biofilm formation on hexadecane between 30 and 10 °C could be attributed to varying degrees of adhesion resulting from differences of the physical state of the

substrate (either liquid or solid depending on the temperature). Planktonic growth on lactate as a substrate was faster at 30 °C than at 10 °C, but the yield of cells was similar in both conditions (Fig. S1, available in the online Supplementary Material). These results strongly suggest that the differences in biofilm formation observed when the bacteria are grown in the presence of hexadecane substrate are unlikely to be due to a faster growth.

On paraffin, the biofilm formation was delayed at 10 °C compared to 30 °C but, once initiated, the biofilm formation rates and yields were similar at both temperatures. This indicates that *Mh* cells in biofilm have good access to paraffin at all tested temperatures. The observations concerning the biofilm production on paraffin were confirmed by CLSM experiments. According to the values of biofilm biovolume, the decrease in temperature delayed the biofilm formation and once the biofilm became established, the number of total cells embedded was stable (Table 2). Moreover, a difference in the structure of the biofilm resulting from growth temperature was observed. The biofilm was found to be less compact (Fig. 2) when developed at 30 °C versus 10 °C, in agreement with a lower substrate surface coverage for an equivalent cell biovolume (Table 2).

Growth temperature influences matrix production and the size and shape of biofilm cells

The influence of temperature on some characteristics of MJ6-1 biofilm was first investigated by SEM experiments on 14-day-old biofilms grown at 10 °C (corresponding to the peak of biofilm production on hexadecane) and 5-day-old

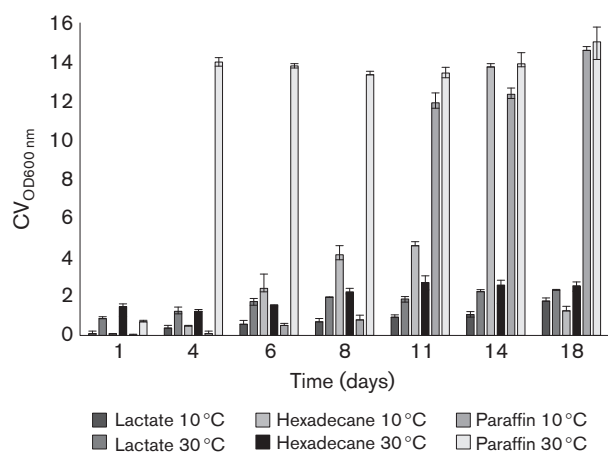


Fig. 1. Biofilm formation of *Mh* grown on lactate, hexadecane or paraffin at 10 or 30 °C quantified by crystal violet staining. Bars of CV_{OD600 nm} mean obtained at each time point for each carbon source at both temperatures. Mean ± SD of nine measurements, three biological replicates and three technical repeats for each.

Table 2. Characteristics of biofilms of *Mh* grown on paraffin at 10 or 30 °C and observed by confocal laser scanning microscopy

Growth duration (day)	Biovolume (μm^3) after growth at		Substrate coverage (%) after growth at	
	10 °C	30 °C	10 °C	30 °C
1	$1.2 \cdot 10^3 \pm 7 \cdot 10^2$	$6.0 \cdot 10^5 \pm 2.1 \cdot 10^4$	0.0±0.0	21.2±0.6
2	$3.2 \cdot 10^4 \pm 1.4 \cdot 10^4$	$1.8 \cdot 10^6 \pm 6.4 \cdot 10^4$	0.8±0.3	40.3±1.2
5	$1.0 \cdot 10^6 \pm 1.0 \cdot 10^5$	$2.2 \cdot 10^6 \pm 8.3 \cdot 10^4$	20.0±0.7	42.0±0.3
9	$1.8 \cdot 10^6 \pm 9.8 \cdot 10^4$	$2.3 \cdot 10^6 \pm 4.9 \cdot 10^4$	66.6±1.7	42.4±1.6
13	$2.2 \cdot 10^6 \pm 6.9 \cdot 10^4$	$2.4 \cdot 10^6 \pm 4.0 \cdot 10^4$	64.1±1.3	46.7±1.1
20	$2.3 \cdot 10^6 \pm 7.4 \cdot 10^4$	$2.6 \cdot 10^6 \pm 1.1 \cdot 10^5$	72.7±3.6	37.9±2.3

The biovolume and the substrate coverage were performed as described in the Methods section. Mean±SD of four results.

biofilms grown at 30 °C (corresponding to a late-grown biofilm at 30 °C, as illustrated by the steady state obtained on paraffin). *Mh* did not produce a matrix when grown on lactate, whereas it produced a light visible matrix when grown at 10 °C on both alkanes (Fig. 3). The largest amount of extracellular matrix was clearly obtained with both alkanes at 30 °C. In the case of the paraffin substrate, the matrix can explain the difference in the biofilm structure between 10 °C (more compact) and 30 °C (Table 2, Fig. 2). Consistently, it was shown that the extracellular matrix of biofilm of *Mh* SP17 grown on alkane at 30 °C is largely composed of proteins that are mandatory for biofilm formation and alkane utilization [33]. The biofilm extracellular matrix is viscoelastic gel, the composition and mechanical properties of which can vary greatly according to environmental factors, including temperature [34]. Also, a correlation between increased matrix production and temperature is sometimes observed for biofilms formed on inert surfaces [35]. During HOC uptake, the matrices are important as they may perform several roles: (i) they can enable adhesion of the biofilms to the nutritious interface; (ii) they can accumulate biosurfactants that contribute to hydrocarbon uptake by substrate emulsification or pseudo-solubilization [11]; and (iii) they can limit the diffusion of nutrients to biofilm-embedded cells. It can be noted that the level of biofilm produced and the

accumulation of lipid storage inclusions, likely occurring during nutrient limitation, were found to be independent of the presence of an extracellular matrix as visualized by SEM. The morphology of biofilm-embedded cells also varied according to the substrate and the temperature (Fig. 3). Bacteria appeared crumpled when grown at 30 °C but not at 10 °C, suggesting that the external membrane of *Mh* could have different properties depending on the temperature. It is well-known that bacteria may adapt the fatty acid and protein composition of their membrane in order to maintain its fluidity and exchanges [36]. When grown on solid hydrocarbon (hexadecane at 10 °C or paraffin at both temperatures), *Mh* exhibited a swollen appearance. This was not observed when bacteria were grown either on lactate at both temperatures or at 30 °C on hexadecane. This could be in relation to the fact that *Mh* SP17 can store lipids within intra-cytoplasmic inclusions [20]. When cells were grown at 30 °C with hexadecane as the sole carbon source, they frequently presented visible hollows at their surface. In the case of *Pseudomonas*, similar images were interpreted as a disruption of the surface membranes [37], allowing the internalization of small biosurfactant-covered hydrocarbon droplets [11].

Finally, according to SEM observations, the bacteria appeared elongated when grown at 10 °C. The temperature-dependent length of *Mh* SP17 was confirmed by CLSM experiments on the JM1 strain, where cells were observed directly without dehydration. The rod-shaped bacteria were longer when grown at 10 °C (lengths 5.00 ± 0.07 and $3.87 \pm 0.07 \mu\text{m}$) compared to 30 °C (lengths 3.48 ± 0.2 and $3.04 \pm 0.06 \mu\text{m}$) for lactate or hexadecane as the growth substrate, respectively. When grown on paraffin, bacteria appeared as rods when grown at 10 °C (length $3.39 \pm 0.07 \mu\text{m}$), whereas they were ovoid when grown at 30 °C (max length $3.70 \pm 0.10 \mu\text{m}$). The greater size at lower temperature was previously observed in the literature [38], and can be correlated to the increase of adherence ability with lower temperature, as observed, for example, for a *Pseudomonas* strain grown on liquid eicosane [39]. Thus, a low temperature may facilitate adhesion to the interface, resulting in an increase in the surface-exchange area and a compensation for the decrease of temperature-dependent nutrient uptake.

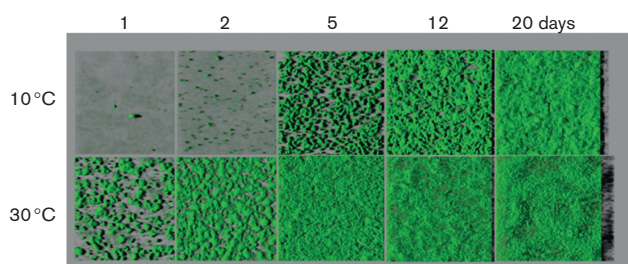


Fig. 2. Three-dimensional reconstructions of *Mh* biofilms grown on paraffin at 10 or 30 °C from confocal laser scanning microscopy z-stack images. The images are representatives of three biological replicates in which we analysed four z-stack images. When applicable, the virtual shadow projection is presented on the right. The grey bar represents 50 μm .

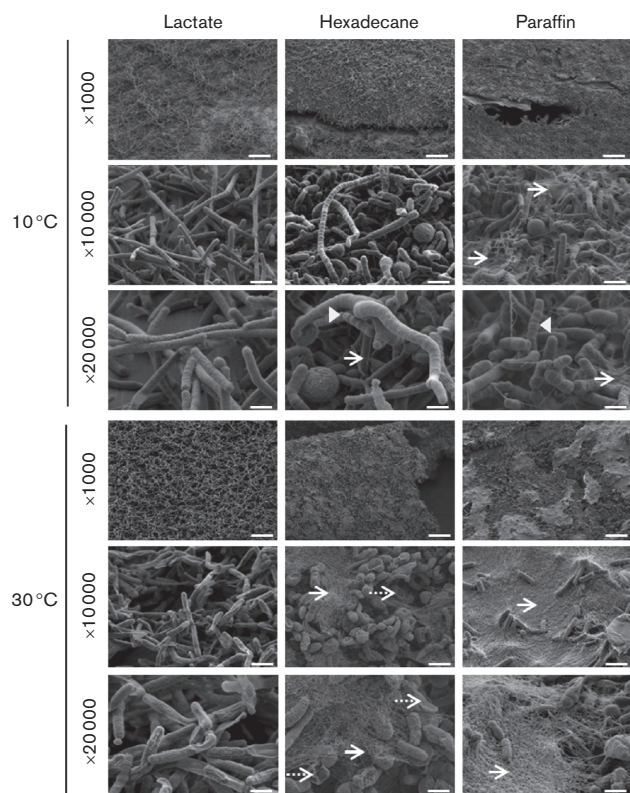


Fig. 3. Scanning electron microscopy micrographs of *Mh* grown on lactate, hexadecane or paraffin at 10 or 30 °C. Biofilm matrices, hollows and swellings in cells are indicated by arrows, dotted arrows and arrowheads, respectively. The bars represent 15, 1.5 and 0.75 μm for magnifications of $\times 1000$, $\times 10000$ and $\times 20000$, respectively.

Growth temperature influences carbon storage

TEM observations were performed on bacterial sections in the different growth conditions to determine whether the blisters observed on cells when grown on solid hydrocarbons were related to intra-cytoplasmic inclusions. The whole population (i.e. biofilm-embedded cells and planktonic cells) was first analysed in mixture as described in the Methods sections. At 10 °C, large amounts of circular and fibre-shaped inclusions were observed in hexadecane- and paraffin-grown bacteria as compared to the small amount of circular inclusions from lactate-grown cells (Fig. 4). In bacteria grown at 30 °C, we observed increasing amounts of inclusions on lactate-grown cells, followed by hexadecane- and, lastly, paraffin-grown cells with the latter being similar to the amount observed at 10 °C on hexadecane- and paraffin-grown bacteria. In addition, we observed a few electron-dense granules, especially when bacteria were grown on hexadecane at 10 °C (Fig. 4). Similar granules, described as polyphosphate granules, have already been observed in marine bacteria [40]. An increase in lipid inclusions was generally found in previous studies with a decrease in growth temperature. For example, two isolates of *Pseudomonas* synthesized and accumulated more polyhydroxyalkanoates at 4 °C than 20 °C when grown

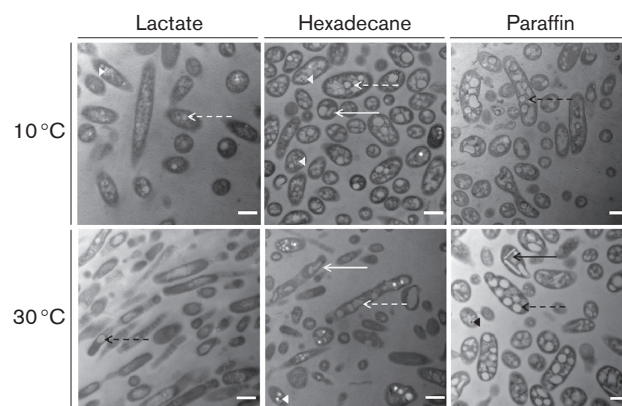


Fig. 4. Transmission electron microscopy micrographs of planktonic and biofilm cells of *Mh* grown on lactate, hexadecane or paraffin at 10 or 30 °C. Rounded inclusions and fibre-shaped inclusions are indicated with dotted or solid arrows, respectively. Electron dense granules are represented by arrowheads. The bars represent 1 μm .

on a soluble substrate, likely due to modifications in enzyme metabolism [40]. Another *Pseudomonas* strain exhibited higher wax ester accumulation when grown on liquid eicosane at lower temperature [39], concomitantly with a higher cell adhesion capacity. Our findings indicate that *Mh* follows this general trend, but they also point out that conditions leading to the highest lipid accumulation are the same as those leading to higher biofilm formation. Klein *et al.* [20] hypothesized that biofilm promotes carbon access on the one hand, but also limits the diffusion of nutrients from the aqueous medium on the other hand. As unfavourable growth conditions, such as nitrogen limitation, are known to enhance intra-cytoplasmic lipids accumulation [12, 41], the biofilm would result in an excess of carbon, stored as cytoplasmic inclusions. In our study, the smaller amount of lipid inclusions observed within cells on hexadecane at 30 °C is in agreement with the hypothesis of a continuous renewing of biofilms and with an absence of nutrient limitation within thin biofilm. In addition, detached cells may quickly consume their intra-cytoplasmic lipid stores, as observed for nutrient-limited cells of *Rhodococcus* [42]. Vaysse *et al.* [24] showed that *Mh* SP17 cells, dispersed from a hexadecane-supported biofilm, exhibited a strongly different protein profile compared to biofilm cells and rapidly degraded intra-cytoplasmic wax ester inclusions that were accumulated during sessile growth. This was correlated to an increased ability of detached cells to reinitiate a new biofilm formation cycle.

The shape of the bacteria cells and the inclusions were also observed by CLSM using double-fluorescent staining with BODIPY and Syto61 for biofilm-embedded cells grown at 30 °C on paraffin (Fig. 6). The BODIPY staining of the inclusions showed that they contained lipid, most likely wax ester, as reported in the literature [20, 43]. After one day, the bacteria were rods with small lipid inclusions. Over time, the lipid inclusions grew, as confirmed by the

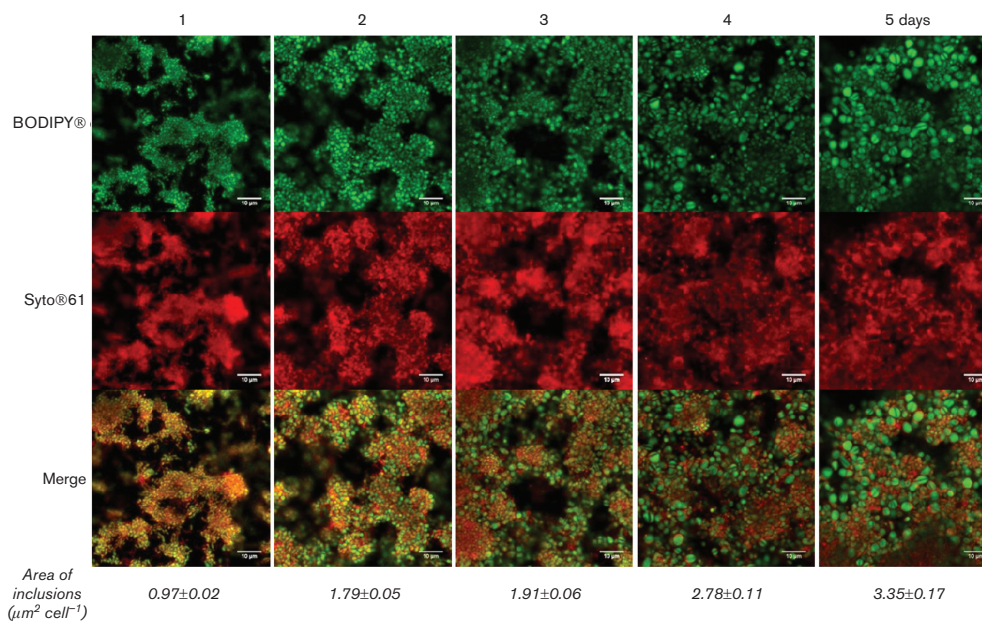


Fig. 5. Confocal laser scanning microscopy images of biofilm cells of *Mh* grown on paraffin at 30°C from day 1 to day 5. The lipid inclusion areas (mean±SD of 50 cells) are indicated at the bottom of the images and were measured from images using BodiPy staining (represented in green on images). The images are representative of three biological replicates in which we analysed four z-stack images. The bars represent 10 µm.

measurement of the lipid inclusion areas (Fig. 5). The mechanism for the formation of lipid storage within prokaryotic cells is described by small lipid droplets that merge to become membrane-bound lipid pre-bodies before being released in the cytoplasm [12], which could explain the cell enlargement. As a consequence, the shapes of the bacteria were modified. Conversely, the growth on paraffin enlarged the cells at 30°C, probably because of a significant intracellular accumulation of lipids, resulting from an imbalance between a rapid substrate uptake and its low metabolization. To further observe cell inclusions and their repartition in cells throughout the biofilm depth, a TEM experiment was performed on the *in situ* biofilm-embedded cells in the case of paraffin incubated at 30°C (5 days), which produced the highest matrix level and the most cohesive biofilm. Cells appeared more densely packed at the bottom of the biofilm (Fig. 6). Cells with several fibre-like or round inclusions (as observed in Fig. 4) were found throughout the depth of the biofilm and large cells filled with inclusions were observed at the surface. The matrix is likely filling (at least partially) the spaces between cells observed in the structured biofilms.

Conclusion

This study provides evidence for temperature being an important factor in the *Mh* adaptation for hydrocarbon uptake. The temperature impacted on the biofilm lifecycle (formation/maturation/detachment) of *Mh* on alkanes in relation to the carbon source properties (solid or liquid). Moreover, it impacted on both the bacterial cells of the biofilm (length, shape and lipid inclusions) and the matrix

production. Part of the observed effects of temperature can most likely be linked to its influence on the physical state of the substrate/substratum. Independently of the temperature, biofilm formation was shown to be mainly for solid hydrocarbon degradation. On the whole, *Mh* is able to adapt and use alkanes as a carbon source when liquid or solid, and under low and intermediate sub-sea water temperature. This opens the way for further studies to decipher the exact

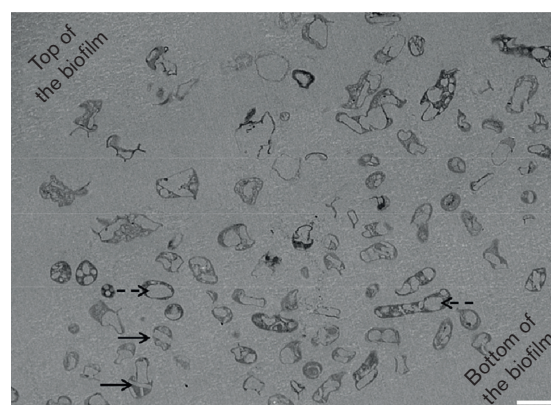


Fig. 6. Transmission electron microscopy micrographs of *in situ* biofilm cells of *Mh* grown on paraffin at 30°C. Bacteria with round or fibre-shaped inclusions are indicated with dotted and solid arrows, respectively. The bar represents 2 µm.

mechanisms of alkane uptake in order to use *Mh* and its relatives in bioremediation of polluted areas.

Funding information

This work was supported by the National Program ANR, project 11 BSV7 002 01 'AD HOC'.

Acknowledgements

We gratefully thank the MIMA2 imaging platform for the contribution to the acquisition of microscopic images. We thank Gabrielle Moulin from AgroParisTech (Massy, France) for her assistance and advice in microscopy studies, and Vincent Contremoulins from Institut Jacques Monod (Paris, France) for his help with CLSM image analysis. We warmly thank Devon Kavanaugh and Mark Reuter from the Institute of Food Research (Norwich, UK) for the English revision.

Conflicts of interest

The authors declare that there are no conflicts of interest.

References

- Scoma A, Yakimov MM, Boon N. Challenging oil bioremediation at deep-sea hydrostatic pressure. *Front Microbiol* 2016;7:3.
- Golyshin PN, Martins dos Santos VA, Kaiser O, Ferrer M, Sabirova YS et al. Genome sequence completed of *Alcanivorax borkumensis*, a hydrocarbon-degrading bacterium that plays a global role in oil removal from marine systems. *J Biotechnol* 2003;106:215–220.
- Yakimov MM, Timmis KN, Golyshin PN. Obligate oil-degrading marine bacteria. *Curr Opin Biotechnol* 2007;18:257–266.
- Bouchez-Naitali M, Rakatozafy H, Marchal R, Leveau JY, Vandecasteele JP. Diversity of bacterial strains degrading hexadecane in relation to the mode of substrate uptake. *J Appl Microbiol* 1999;86:421–428.
- Grimaud R. Biofilm development at interfaces between hydrophobic organic compounds and water. In: Timmis KN (editor). *Handbook of Hydrocarbons and Lipid Microbiology*. Berlin: Springer; 2010. pp. 1491–1499.
- Baldi F, Ivosevic N, Minacci A, Pepi M, Fani R et al. Adhesion of *Acinetobacter venetianus* to diesel fuel droplets studied with *in situ* electrochemical and molecular probes. *Applied Environ Microbiol* 1999;65:2041–2048.
- Bouchez-Naitali M, Blanchet D, Bardin V, Vandecasteele JP. Evidence for interfacial uptake in hexadecane degradation by *Rhodococcus equi*: the importance of cell flocculation. *Microbiology* 2001; 147:2537–2543.
- Whyte LG, Slagman SJ, Pietrantonio F, Bourbonniere L, Koval SF et al. Physiological adaptations involved in alkane assimilation at a low temperature by *Rhodococcus* sp. strain Q15. *Appl Environ Microbiol* 1999;65:1–2968.
- van Hamme JD, Singh A, Ward OP. Physiological aspects. Part 1 in a series of papers devoted to surfactants in microbiology and biotechnology. *Biotechnol Adv* 2006;24:4–620.
- Heipieper HJ, Cornelissen S, Pepi M. Surface properties and cellular energetics of bacteria in response to the presence of hydrocarbons. In: Timmis KN (editor). *Handbook of Hydrocarbons and Lipid Microbiology*. Berlin: Springer; 2010. pp. 1615–1624.
- Cameotra SS, Singh P. Synthesis of rhamnolipid biosurfactant and mode of hexadecane uptake by *Pseudomonas* species. *Microb Cell Fact* 2009;8:16.
- Wältermann M, Steinbüchel A. Neutral lipid bodies in prokaryotes: recent insights into structure, formation, and relationship to eukaryotic lipid depots. *J Bacteriol* 2005;187:3607–3619.
- Deppe U, Richnow HH, Michaelis W, Antranikian G. Degradation of crude oil by an arctic microbial consortium. *Extremophiles* 2005;9: 461–470.
- Edwards KJ, Rogers DR, Wirsén CO, Mccollom TM. Isolation and characterization of novel psychrophilic, neutrophilic, Fe-oxidizing, chemolithoautotrophic alpha- and gamma-proteobacteria from the deep sea. *Appl Environ Microbiol* 2003;69:2906–2913.
- Handley KM, Lloyd JR. Biogeochemical implications of the ubiquitous colonization of marine habitats and redox gradients by *Marinobacter* species. *Front Microbiol* 2013;4:6.
- Kim BY, Weon HY, Yoo SH, Kim JS, Kwon SW et al. *Marinobacter koreensis* sp. nov., isolated from sea sand in Korea. *Int J Syst Evol Microbiol* 2006;56:2653–2656.
- Takai K, Moyer CL, Miyazaki M, Nogi Y, Hirayama H et al. *Marinobacter alkaliphilus* sp. nov., a novel alkaliphilic bacterium isolated from subseafloor alkaline serpentine mud from Ocean Drilling Program site 1200 at South Chamorro Seamount, Mariana Forearc. *Extremophiles* 2005;9:17–27.
- Al-Mailem DM, Eliyas M, Khanafer M, Radwan SS. Biofilms constructed for the removal of hydrocarbon pollutants from hypersaline liquids. *Extremophiles* 2015;19:189–196.
- Gauthier MJ, Lafay B, Christen R, Fernandez L, Acquaviva M et al. *Marinobacter hydrocarbonoclasticus* gen. nov., sp. nov., a new, extremely halotolerant, hydrocarbon-degrading marine bacterium. *Int J Syst Bacteriol* 1992;42:568–576.
- Klein B, Grossi V, Bouriat P, Goulas P, Grimaud R. Cytoplasmic wax ester accumulation during biofilm-driven substrate assimilation at the alkane–water interface by *Marinobacter hydrocarbonoclasticus* SP17. *Res Microbiol* 2008;159:137–144.
- Klein B, Bouriat P, Goulas P, Grimaud R. Behavior of *Marinobacter hydrocarbonoclasticus* SP17 cells during initiation of biofilm formation at the alkane–water interface. *Biotechnol Bioeng* 2010;105: 461–468.
- Vaysse PJ, Prat L, Mangenot S, Cruveiller S, Goulas P et al. Proteomic analysis of *Marinobacter hydrocarbonoclasticus* SP17 biofilm formation at the alkane–water interface reveals novel proteins and cellular processes involved in hexadecane assimilation. *Res Microbiol* 2009;160:829–837.
- Mounier J, Camus A, Mitteau I, Vaysse PJ, Goulas P et al. The marine bacterium *Marinobacter hydrocarbonoclasticus* SP17 degrades a wide range of lipids and hydrocarbons through the formation of oleolytic biofilms with distinct gene expression profiles. *FEMS Microbiol Ecol* 2014;90:816–831.
- Vaysse PJ, Sivadon P, Goulas P, Grimaud R. Cells dispersed from *Marinobacter hydrocarbonoclasticus* SP17 biofilm exhibit a specific protein profile associated with a higher ability to reinitiate biofilm development at the hexadecane–water interface. *Environ Microbiol* 2011;13:737–746.
- de Oliveira DC, Fernandes Júnior A, Kaneno R, Silva MG, Araújo Júnior JP et al. Ability of *Salmonella* spp. to produce biofilm is dependent on temperature and surface material. *Foodborne Pathog Dis* 2014;11:478–483.
- Nesse LL, Sekse C, Berg K, Johannesen KC, Solheim H et al. Potentially pathogenic *Escherichia coli* can form a biofilm under conditions relevant to the food production chain. *Appl Environ Microbiol* 2014;80:2042–2049.
- Uhlich GA, Chen CY, Cottrell BJ, Nguyen LH. Growth media and temperature effects on biofilm formation by serotype O157:H7 and non-O157 Shiga toxin-producing *Escherichia coli*. *FEMS Microbiol Lett* 2014;354:133–141.
- Choi KH, Schweizer HP. mini-Tn7 insertion in bacteria with single attTn7 sites: example *Pseudomonas aeruginosa*. *Nat Protoc* 2006;1: 153–161.
- Canette A, Branchu P, Grimaud R, Naitali M. Imaging bacterial cells and biofilms adhering to hydrophobic organic compounds–water interfaces. In: McGenity TJ, Timmis KN and Nogales B (editors). *Hydrocarbon and Lipid Microbiology Protocols Springer Protocols Handbooks*. Heidelberg, Berlin: Springer-Verlag; 2015.
- Sanchez-Vizueté P, Le Coq D, Bridier A, Herry JM, Aymerich S et al. Identification of *ypqP* as a new *Bacillus subtilis* biofilm determinant that mediates the protection of *Staphylococcus aureus* against antimicrobial agents in mixed-species communities. *Appl Environ Microbiol* 2015;81:109–118.

31. de Chaumont F, Dallongeville S, Chenouard N, Hervé N, Pop S et al. Icy: an open bioimage informatics platform for extended reproducible research. *Nat Methods* 2012;9:690–696.
32. Schindelin J, Arganda-Carreras I, Frise E, Kaynig V, Longair M et al. Fiji: an open-source platform for biological-image analysis. *Nat Methods* 2012;9:676–682.
33. Ennouri H, D'Abzac P, Hakil F, Branchu P, Naïtali M et al. The extracellular matrix of the oleolytic biofilms of *Marinobacter hydrocarbonoclasticus* comprises cytoplasmic proteins and T2SS effectors that promote growth on hydrocarbons and lipids. *Environ Microbiol* 2017;19:159–173.
34. Flemming H-C, Wingender J. The biofilm matrix. *Nat Rev Microbiol* 2010;7:3–633.
35. Abdallah M, Chataigne G, Ferreira-Theret P, Benoliel C, Drider D et al. Effect of growth temperature, surface type and incubation time on the resistance of *Staphylococcus aureus* biofilms to disinfectants. *Appl Microbiol Biotechnol* 2014;98:2597–2607.
36. Shivaji S, Prakash JS. How do bacteria sense and respond to low temperature? *Arch Microbiol* 2010;192:85–95.
37. Hua F, Wang H. Uptake modes of octadecane by *Pseudomonas* sp. DG17 and synthesis of biosurfactant. *J Appl Microbiol* 2012;112:7–37.
38. Chavant P, Martinie B, Meylheuc T, Bellon-Fontaine MN, Hebraud M. *Listeria monocytogenes* LO28: surface physicochemical properties and ability to form biofilms at different temperatures and growth phases. *Appl Environ Microbiol* 2002;68:728–737.
39. Husain DR, Goutx M, Acquaviva M, Gilewicz M, Bertrand J-C. The effect of temperature on eicosane substrate uptake modes by marine bacterium *Pseudomonas nautica* strain 617: relationship with the biochemical content of cells and supernatants. *World J Microbiol Biotechnol* 1997;13:587–590.
40. Alvarez HM, Pucci OH, Steinbüchel A. Lipid storage compounds in marine bacteria. *Appl Microbiol Biotechnol* 1997;47:132–139.
41. Ishige T, Tani A, Takabe K, Kawasaki K, Sakai Y et al. Wax ester production from n-alkanes by *Acinetobacter* sp. strain M-1: ultrastructure of cellular inclusions and role of acyl coenzyme A reductase. *Appl Environ Microbiol* 2002;68:1192–1195.
42. Alvarez HM, Kalscheuer R, Steinbüchel A. Accumulation and mobilization of storage lipids by *Rhodococcus opacus* PD630 and *Rhodococcus ruber* NCIMB 40126. *Appl Microbiol Biotechnol* 2000;54:218–223.
43. Manilla-Pérez E, Reers C, Baumgart M, Hetzler S, Reichelt R et al. Analysis of lipid export in hydrocarbonoclastic bacteria of the genus *Alcanivorax*: identification of lipid export-negative mutants of *Alcanivorax borkumensis* SK2 and *Alcanivorax jadensis* T9. *J Bacteriol* 2010;192:643–656.

Edited by: R. E. Parales and I. Martin-Verstraete

Five reasons to publish your next article with a Microbiology Society journal

1. The Microbiology Society is a not-for-profit organization.
2. We offer fast and rigorous peer review – average time to first decision is 4–6 weeks.
3. Our journals have a global readership with subscriptions held in research institutions around the world.
4. 80% of our authors rate our submission process as 'excellent' or 'very good'.
5. Your article will be published on an interactive journal platform with advanced metrics.

Find out more and submit your article at microbiologyresearch.org.